CrossMark

REVIEW ARTICLE

Recent Advances for Rapid Identification of Chemical Information of Muscle Foods by Hyperspectral Imaging Analysis

Yu-Nan Chen[1,2] · Da-Wen Sun[1,2,3] ⑩ · Jun-Hu Cheng[1,2] · Wen-Hong Gao[1,2]

Abstract Muscle foods play an important role in providing a vital source of high-quality protein, amino acids and vitamin for human health. Chemical composition is one of the most vital information of muscle foods, which directly relates to the quality of pork, beef, chicken, fish and other meats. Therefore, it is significant to identify the chemical information of muscle foods for the purpose of controlling the quality and safety of meat. Hyperspectral imaging can obtain spectral and spatial information of targets simultaneously and has been developed for rapid and nondestructive determination and identification of chemical information of muscle foods. This review focuses on recent applications of hyperspectral imaging technology for the measurement and analysis of chemical composition of muscle foods, including moisture content, fat and fatty acid, pH, protein content, pigment, salt content and freshness attributes. The fundamentals of hyperspectral imaging as well as future development trends are also presented and discussed.

Keywords Hyperspectral imaging · Chemical composition · Muscle foods · Seafood products · Optimal wavelengths · Prediction models

✉ Da-Wen Sun
dawen.sun@ucd.ie;
http://www.ucd.ie/refrig; http://www.ucd.ie/sun

1 College of Food Science and Engineering, South China University of Technology, Guangzhou 510641, China

2 Academy of Contemporary Food Engineering, South China University of Technology, Guangzhou Higher Education Mega Center, Guangzhou 510006, China

3 Food Refrigeration and Computerized Food Technology, Agriculture and Food Science Centre, University College Dublin, National University of Ireland, Belfield, Dublin 4, Ireland

Introduction

Generally speaking, muscle foods such as pork, beef, lamb, chicken and seafood are one of the most vital part of people's daily diet, as they are important sources of high-quality protein, amino acids and vitamin. In addition, they are highly perishable. With the development of living standard, customers pay more and more attention to the quality and safety of food. Therefore, besides the need for reservation techniques and methods such as cooling [1–4], freezing [5] and drying [6, 7] to provide superior quality meat and meat products, the meat industry also require modern reliable tools for quality and safety assurance. The quality attributes of muscle foods generally consist of physical attributes, biological attributes and chemical attributes [8], among which chemical composition has a major impact on the quality.

Traditionally, chemical composition is usually identified by chemical analysis methods, even by experienced assessors, for instance, a solvent-based method for measuring the total fat content in meat [9], a portable pH meter or a surface electrode for measuring the pH value of salmon flesh [10] and the marbling score assessed by trained assessors according to a referenced table for estimating the intramuscular fat content of meat [11]. However, the above-mentioned methods are time-consuming, destructive, tedious and demanding, which are not suitable for real-time or on-line operations. With the target of giving consumers more reliance on current environment of food, objective, noninvasive and nondestructive techniques are needed for the rapid identification of chemical composition of muscle foods.

In recent years, a number of nondestructive and objective technologies for measuring the chemical properties of muscle foods have emerged, including ultrasound imaging

(UI), fluorescence imaging (FI), visible (VIS) and near-infrared (NIR) spectroscopy and computer vision [12–15], among which spectroscopic and imaging are two important technologies available. The spectral data obtained by VIS–NIR spectroscopy cover 380–2526 nm and provide the chemical information of samples. Meanwhile, imaging techniques focus on collecting external information of samples, such as shape, size, color and texture, so that it is usually used for rapid identification of different visual quality parameters based on spatial information. However, these methods have their own disadvantages; for instance, UI can be affected by operators easily and is only available for detecting specific parts of objects [16], FI can only detect some specific materials related to fluorescence [17], while NIR spectroscopy and computer vision can only obtain spectral or spatial data, respectively. More specifically, spectral information obtained by spectroscopy alone is not able to illustrate the concentration gradients in the entire tested sample, because it uses information of a specific part of the specimen analyzed to represent the average value of the specimen; while only using imaging techniques, internal attributes such as moisture, fat and protein cannot be identified quantitatively.

On the other hand, by the integration of two popular techniques, spectroscopic and imaging, into one system, hyperspectral imaging is able to obtain both abundant contiguous spectral bands and spatial distribution information of objects simultaneously [18–28]. Originally, hyperspectral imaging was applied in the field of remote sensing, such as marine monitoring, detecting of forest fire, and exploring geological and mineral resources [29]. Over the past few years, the applications of hyperspectral imaging technology have been extended to the area of assessing food quality and safety [30–33], including identifying chemical composition of muscle foods.

Up to now, there are some reviews about the applications of hyperspectral imaging in measuring quality and safety of muscle foods [25, 34, 35]; however, no reviews are available focusing on muscle foods chemical composition. Therefore, this paper is aimed at summarizing the applications of hyperspectral imaging in this domain.

Fundamentals of Hyperspectral Imaging

Fundamental Devices and Software

There are three available types of hyperspectral imaging configurations, including tunable filter, whiskbroom and push-broom, with the push-broom being the most common configuration for meat applications. The difference between three configurations are in the way of scanning, among which tunable filter is conceptually called wavelength scanning, while the other two configurations are called spectral scanning, since samples are scanned point to point (whiskbroom) or line to line (push-broom) in the spatial domain, respectively [19]. Figure 1 shows a typical push-broom hyperspectral imaging system, consisting of a light source, a motor, a wavelength dispersion device or spectrograph, a two-dimensional detector or camera, and a computer. It is worth mentioning that imaging spectrograph acts the same role of human eyes, but its available scanning range contains ultraviolet, visible and near-infrared regions (300–2600 nm), overcoming the limitation of the identification of only red, green and blue (RGB) bands by human eyes [25]; another function of imaging spectrograph is to distribute the wide bands into different wavelengths and disperse the acquired light onto a two-dimensional charge-coupled device (CCD) detector array [19], while the computer system with relevant control and process software is mainly for further analysis of targets by controlling the hyperspectral imaging system, including motor rate, exposure time and wavelength range, and accomplishing the further process procedure, such as the calibration and storage of images.

In addition to hardware, software developed to make the transfer of technology successfully plays a significant role in the application of hyperspectral imaging. So far, several effective software for processing hyperspectral data have been implemented widely, including ENVI, MATLAB, Unscrambler and others. ENVI is a dedicated software bundled with a variety of image processing algorithms available, which are usually used for processing hyperspectral images, including filtering, calibration and extracting the regions of interest (ROIs); meanwhile MATLAB, a fourth-generation computing language, has powerful capacity in aspects of algorithms development, models establishment, data and images analysis and visualization [37]. However, more software needs to be developed for practical and industrial application, as the development of software is behind that of hardware [16].

Image Data Processing

Because of the fusion of spectroscopy and computer vision, the information contained in hyperspectral images is a three-dimensional data cube, named "hypercube" or "spectral cube" [37], including two-dimensional spatial information (x, y) and one-dimensional spectral information (λ). The relationship between spatial dimension and spectral dimension is presented in Fig. 2. The resulting characteristic spectra play the role of fingerprint for identifying chemical composition, and the images provide geometrical features of samples, including color, shape, texture, appearance.

Camera

Spectrograph

Lens

Computer system

Illumination

Motor

Sample position

Translation stage

Fig. 2 Relationship between spatial dimension and spectral dimension

Image at λ_i

Pixel spectrum at (x_i, y_i)

Image at λ'_i

Reflectance

(x_i, y_i)

λ_i Wavelength λ'_i

(x_i, y_i)
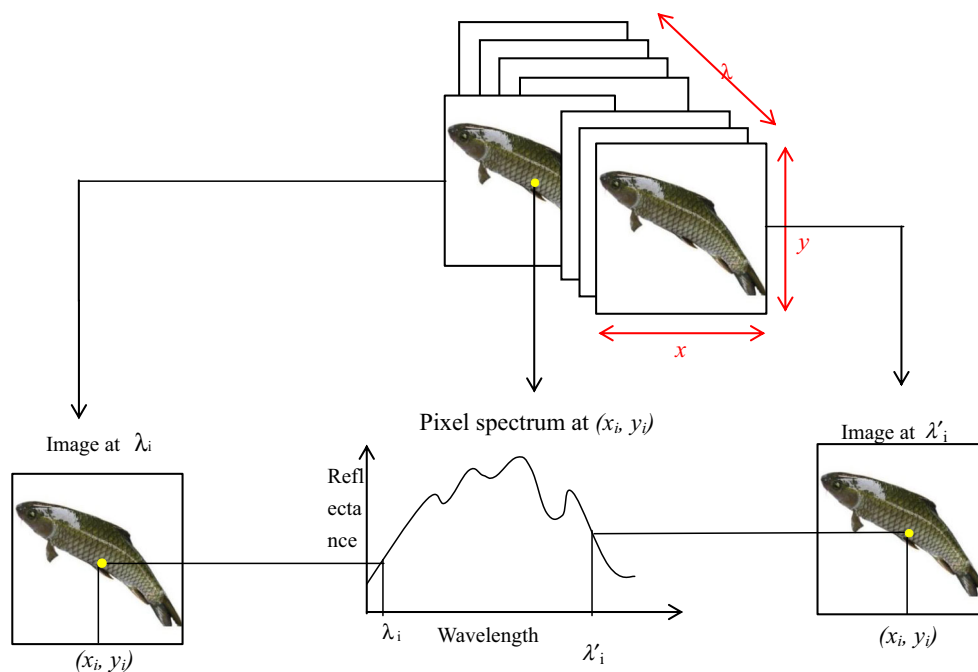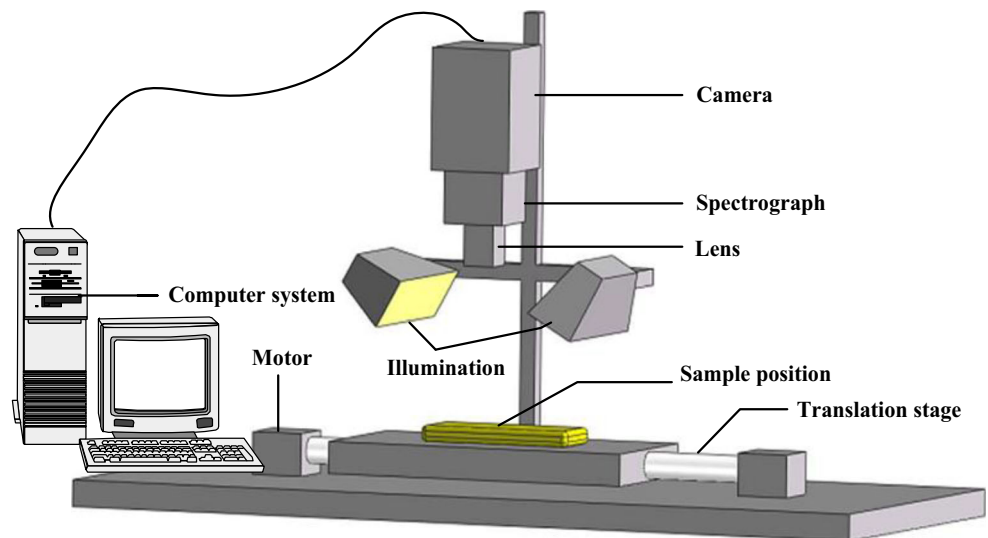
After collecting hyperspectral images by point scanning, line scanning, area scanning or the single shot method, abundant available spectral information of targets can be extracted, certainly along with some redundant information having negative impacts on calibration. The redundant data include collinear information, light scattering, even stripe and random noise produced by hyperspectral equipment and other random factors, which carry useless spectral information and disturbing the extraction of characteristic spectrum. Therefore, these invalid data can slow down the efficiency of analysis and have negative effects on

chemical composition prediction. For the purpose of enhancing the predictive ability of model and diminishing different impacts between diverse samples, some spectral preprocessing techniques are applied to calibrate the original spectra, generally including using multiplicative scatter correction (MSC), standard normal variables (SNV), median filter, Fourier transform (FT) and wavelet transforms (WT), among which FT and WT are appropriate for noise reduction and edge detection. MSC works for removing the undesirable information caused by scattering from the data matrix, so that the spectral information

available for detection can be enhanced [38]. And the function of SNV is similar to MSC. After that, calibration of spectra and establishment of models are the two main tasks, normally associated with chemometrics for analyzing the relationship between each pixel in the images and corresponding quality attributes. Among the common chemometric methods, both linear analysis methods, such as principal component regression (PCR), multiple linear regression (MLR) and partial least squares regression (PLSR), and nonlinear analysis methods, such as artificial neural network (ANN) and support vector machine (SVM), can serve for multivariate data processing [39]. It is worth mentioning that PLSR can perform excellently when the matrix of wavelengths has more variables than samples and when the original wavelengths have a high correlation [40]. MLR, an important linear multivariate regression methodology, can provide correlation between spectra and target indexes; however, different from PLSR, it loses efficacy when the number of samples is less than that of variables [37]. ANN, whose operating principle is similar to the way of human brain in processing information, divides the neural network into hundreds of single units (artificial neurons or processing elements) with individual weighted coefficient [41]; however, it lacks in accuracy and universality for each indexes in neural network and system structure, respectively. SVM, a popular supervised learning machine, utilizes SV kernel to translate the variables and dependent variables from input space into a high-dimensional feature space where the relationship between variables can be corresponded to by a linear function [42]. Particularly, least square support vector machine (LS-SVM), an updated version of standard SVM, is widely used for classification and regression tasks in hyperspectral imaging applications. In addition to the above-mentioned chemometrics, simple methods to select the optimal wavelengths should also be considered. Because the target attributes are usually only related to some key wavelengths, so selecting the optimal wavelengths are necessary for the purpose of improving the efficiency of analysis. At present, frequently used selection methods in multispectral wavelengths include regression coefficients (RC) of PLSR, independent component analysis (ICA), principal component analysis (PCA) and genetic algorithm (GA). Details of recent advances in these wavelength selection methods for hyperspectral imaging applications can be found elsewhere [26]. Based on selected wavelengths, simplified models can be established, and then best performance model can be selected to translate spectral data in each pixel into chemical map, which is considered as the most significant function of hyperspectral imaging. Figure 3 illustrates several chemical maps of the thiobarbituric acid (TBA) value [43], K value [44], moisture content [45], pH [46], fat content [47], hydroxyproline values [48] and salt content [49, 50], respectively. Detailed discussion

and analysis about these studies are presented in the sections below. Besides, it is worth mentioning that K value is an important chemical index for evaluating the quality and freshness of muscle foods by reflecting the degradation of nucleotide. Meanwhile, the main procedures of hyperspectral imaging in identification of meat chemical composition are shown in Fig. 4.

Finally, it is worth mentioning the criteria used for evaluating the performance (accuracy, reliability and predictive ability) of models. Generally, the evaluation criteria are associated with statistical references, such as the coefficients of determination and root mean square errors in calibration (R_C^2, RMSEC), cross-validation (R_{CV}^2, RMSECV) and prediction (R_P^2, RMSEP) [52]. R^2 is usually calculated using the following equation:

$$R^2 = \frac{\left[\sum_{i=1}^{n}(x_i - \bar{x})(y_i - \bar{y})\right]^2}{\sum_{i=1}^{n}(x_i - \bar{x})^2 \sum_{i=1}^{n}(y_i - \bar{y})^2} \tag{1}$$

and RMSE can be expressed as follows:

$$\text{RMSE} = \sqrt{\frac{1}{n}\sum_{i=1}^{n}(y_i - x_i)^2} \tag{2}$$

where x_i is the measurement value of target, $\bar{x}$ is the mean value of x_i, y_i is prediction value, and $\bar{y}$ is the mean value of y_i. A satisfactory model should possess higher values of R_C^2, R_{CV}^2 and R_P^2, lower values of RMSEC, RMSECV and RMSEP, even smaller differences between RMSEC, RMSECV and RMSEP. Moreover, it is commonly believed that the performance of a model is poor, acceptable, good and excellent if its R^2 is under 0.66, between 0.66–0.81, between 0.82–0.90 and over 0.9, respectively [53].

Applications

The chemical composition in the muscle foods, such as moisture, protein, fat and pigment, is directly related to the flavor, color and quality of meat, which immediately affect the purchasing desire of consumers. So far, there are a number of studies involving the identification and assessment of the chemical composition of muscle foods by hyperspectral imaging techniques, and Tables 1 and 2 summarize these studies. Most of the studies mentioned in Tables 1 and 2 are introduced in detail in the following sections.

Moisture Content

Moisture, as one of the most important composition in meat, profoundly has relation to the quality of meat, as well as shelf-life and economic profits, as muscle foods are usually sold by weight. During the past few years, hyperspectral imaging as an expeditious emerging and objective
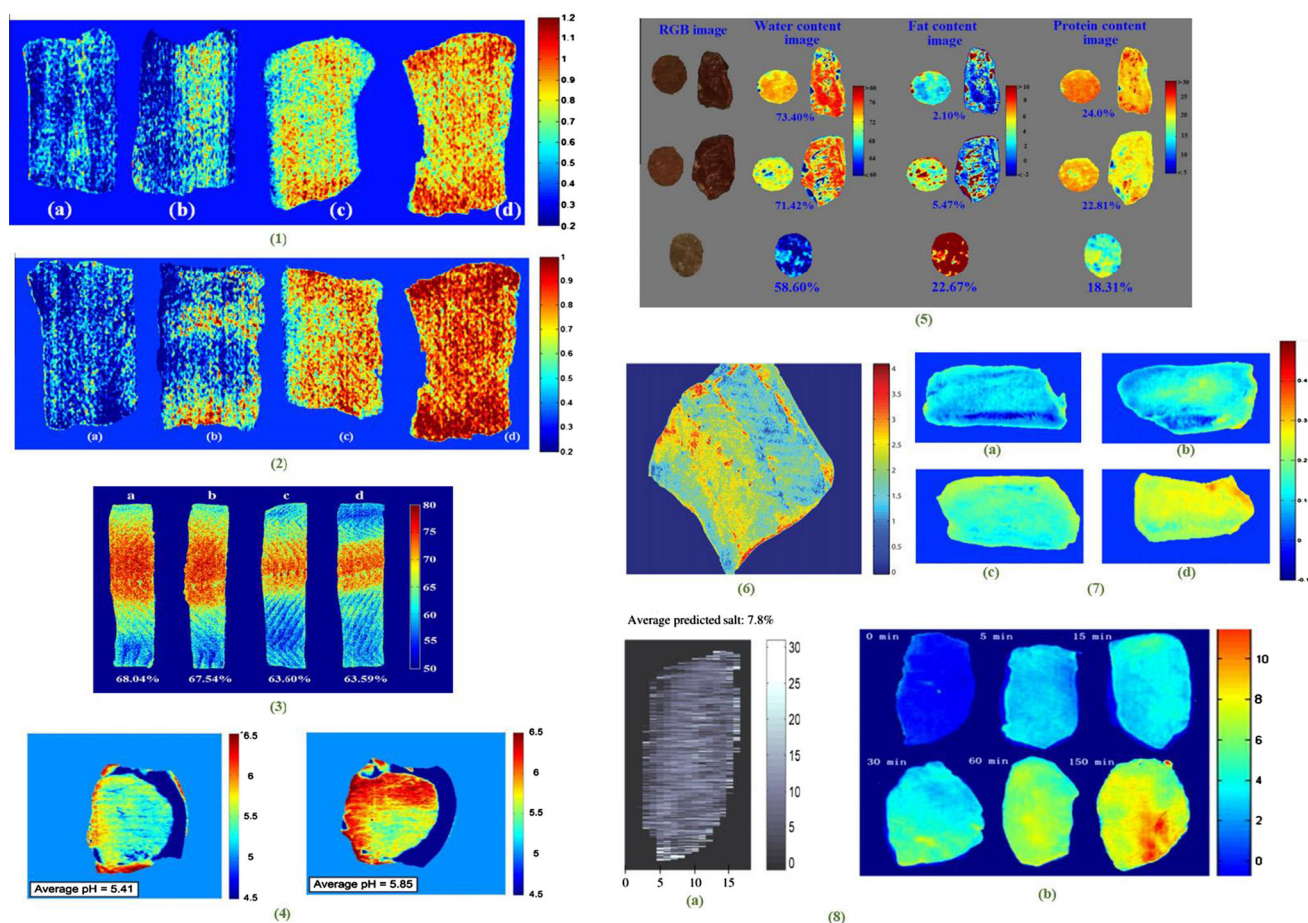
Fig. 3 Chemical maps of hyperspectral images. **1** Chemical maps of TBA value in fish fillets at four different TBA values [43]. **a** TBA = 0.2355 mg/kg; **b** TBA = 0.4602 mg/kg; **c** TBA = 0.9524 mg/kg; **d** TBA = 1.1213 mg/kg. **2** Chemical maps of *K* value in fish fillets at four different *K* values [44]. **a** *K* = 24.2 %; **b** *K* = 45.6 %; **c** *K* = 78.1 %; **d** *K* = 89.8 %. **3** Chemical maps of moisture in salmon fillets at different moisture values [45]. **4** Distribution map for different pH value in pork samples [46]. **5** Chemical maps of water, fat and protein contents resulting from two different samples (first and second rows) and from fat trimmings of beef samples (third row) [47].

6 Visualization of entire salmonids piece with average astaxanthin content of 2.26 μg [51]. **7** Chemical map of chicken meat at four different hydroxyproline values [48]. **a** Hydroxyproline value of 0.065 g/100 g; **b** hydroxyproline value of 0.110 g/100 g; **c** hydroxyproline value of 0.149 g/100 g; **d** hydroxyproline value of 0.268 g/100 g. **8** Chemical maps of salt content in different meat products. **a** 2D distribution within one slice of ham for average salt content of 7.8 % [49]. **b** Distribution map of salt content in a single porcine meat slices at six different salting periods [50]

technology has been widely developed for the moisture content evaluation.

Among various studies, Barbin et al. [18] focused on assessing the moisture content of minced and raw pork using a push-broom hyperspectral imaging system to extract the spectral data between 900 and 1700 nm. PLSR was developed to correlate predictors (spectral data) with responders (measured reference values), and leave-one-out cross-validation (LOOCV) method was employed to build PLSR model with training set under full cross-validation. The final PLSR prediction model, established with seven feature-related wavelengths (927, 950, 1047, 1211, 1325, 1513 and 1645 nm) selected by RC of PLSR, showed R_P^2 of 0.91 and standard error in prediction (SEP) of 0.62 %. In another study, ElMasry et al. [47] developed a push-broom

hyperspectral imaging system to collect the hyperspectral images of fresh beef line by line, in order to determine the moisture content of the samples. In the near-infrared (NIR) range (900–1700 nm), PLSR model was chosen to visualize the moisture of beef with eight key wavelengths (934, 1048, 1108, 1155, 1185, 1212, 1265 and 1379 nm) selected by RC of PLSR, with a satisfying result of R_P^2 of 0.89 and SEP of 0.46 %. Furthermore, a push-broom hyperspectral imaging system, based on the reflectance mode, was applied to evaluate the moisture content in lamb from different breeds and muscles [20]. By extracting the spectral information from the hyperspectral images, PLSR was employed to establish a multivariate calibration model for predicting the moisture content with six wavelengths (960, 1057, 1131, 1211, 1308 and 1394 nm) selected by
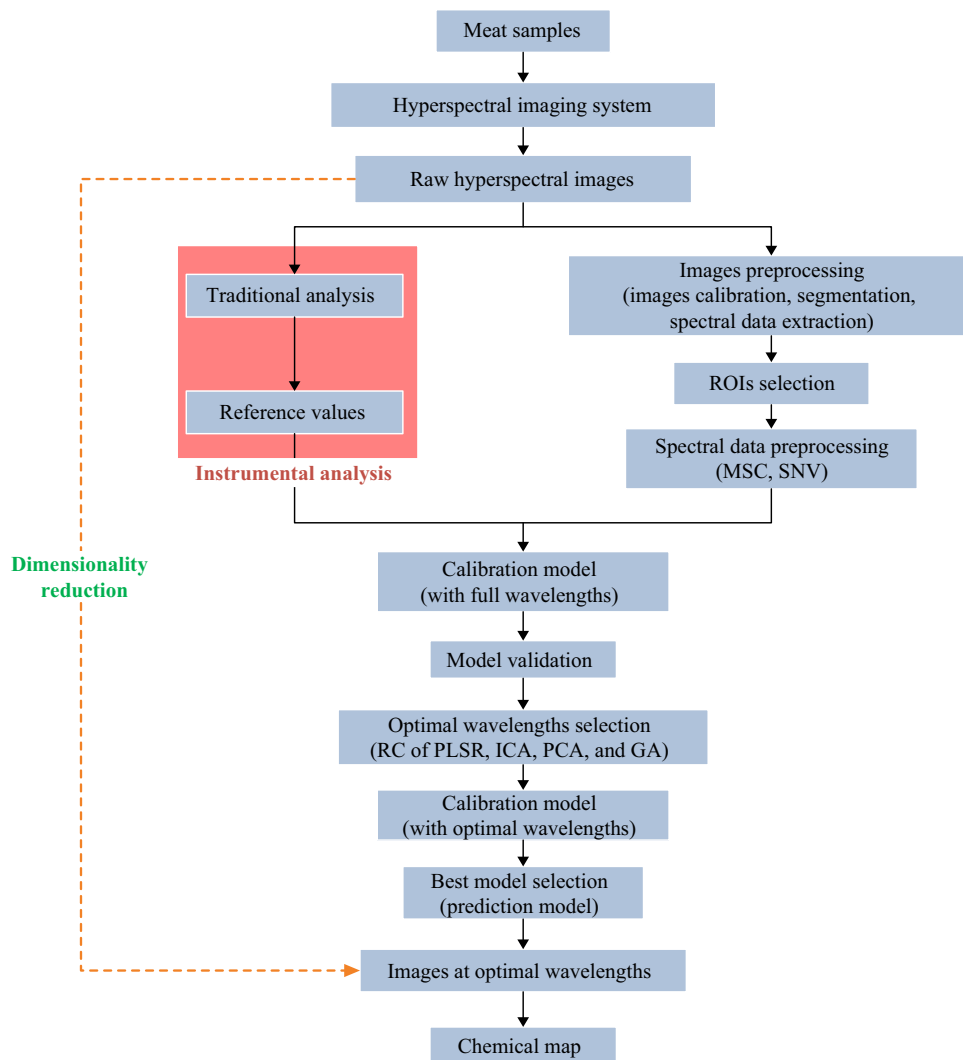
Fig. 4 Main procedures of hyperspectral imaging in identification of meat chemical composition

RC of PLSR. Satisfactorily, the simplified PLSR model showed an encouraging performance in evaluating the moisture of lamb ($R_P^2 = 0.84$ and SEP = 0.57 %).

On the basis of the above results, it is obvious that PLSR is one of the most common and available algorithm for multivariate analysis and models establishment. In addition, the number and location of optimal wavelengths in the above three studies are different, although all selected by RC of PLSR. Compared to the other two studies [18, 47], the model from Kamruzzaman et al. [20] for predicting moisture content in pork performed better. The difference in prediction performance and optimal wavelengths selection may be resulted from different species of meat samples used. In the above three studies, all of the R_P^2 surpassed 0.8, not only showing the reliability of models, but also revealing the potential of hyperspectral imaging technology for predicting the target constituent of objects.

For seafood products, He et al. [45] investigated the feasibility of hyperspectral imaging in determination of moisture content distribution in farmed Atlantic salmons with three spectral ranges, including range I (400–1000 nm), range II (900–1700 nm) and range III (400–1700 nm). Based on the whole spectral information, PLSR models are established for three spectral regions, respectively, and its mean RESMC (1.535 %) and RESMCV (1.648 %) were lower than those reported in a previous study on predicting moisture content in six species fish fillets [71]. In order to improve computational efficiency, He et al. [45] selected several feature-related wavelengths by RC of PLSR and built the simplified models based on three spectral ranges, respectively. The results [45] revealed that the simplified models can replace the models using full spectral wavelengths, as their performances were comparable, and spectral range I showed more reasonable values in industrial

Table 1 Applications of hyperspectral imaging for determination of chemical attributes of poultry meats

Species	Features	Spectral range (nm)	Method	R_P^2/R^2	Reference
Pork	pH	400–1000	FNN	0.303	Qiao et al. [54]
	pH	900–1700	PLSR	0.90	Barbin et al. [46]
	pH	400–1000	PLSR	0.794	Liu et al. [55]
	pH	400–1000	LS-SVM	0.714	Pu et al. [56]
	pH	400–2500	PLSR	0.257	Xie et al. [57]
	Moisture	900–1700	PLSR	0.91	Barbin et al. [18]
	Protein			0.88	
	Fat content			0.93	
	Salt content	400–1000	PLSR	0.912	Liu et al. [50]
			PCA	0.933	
			MLR	0.930	
	Intramuscular fat (IMF) content	900–1700	PLSR	0.920	Liu and Ngadi [11]
	TVB-N	430–960	BP-ANN	0.695	Chen et al. [17, 58]
	TVB-N	400–1100	PLSR	0.90	Kim et al. [59]
Beef	pH	900–1700	PLSR	0.73	ElMasry et al. [19, 60]
	Fat content	1000–2300	PLSR	0.90	Kobayashi et al. [61]
	Fatty acid (saturated and unsaturated)			(0.87, 0.89)	
	Marbling grade	400–1100	MLR	0.92	Li et al. [62]
	Moisture	900–1700	PLSR	0.89	ElMasry et al. [47]
	Protein			0.86	
	Fat content			0.84	
	pigments	400–1000	PLSR	0.953	Xiong et al. [63]
Lamb	pH	900–1700	PLSR	0.65	Kamruzzaman et al. [64]
	Moisture	900–1700	PLSR	0.88	Kamruzzaman et al. [20]
	Protein			0.63	
	fat content			0.88	
	Moisture	900–1700	MLR	0.83	Pu et al. [65]
	protein			0.64	
	fat content			0.90	
Chicken	Moisture content	400-1000	PLSR	0.94	Kandpal et al. [66]
	Hydroxyproline content	400–1000	PLSR	0.73	Xiong et al. [48]
	TBA value	400–1000	PLSR	0.64	Xiong et al. [67]
Goose/Duck	Pigments	400–1000	PLSR	0.953	Xiong et al. [63]

TVB-N total volatile basic nitrogen, *TBA* thiobarbituric acid, *FNN* feed-forward neural network, *PLSR* partial least squares regression, *LS-SVM* least square support vector machine, *PCA* principal component analysis, *MLR* multiple linear regression, *BP-ANN* back-propagation artificial neural network

applications, as it had prediction precision similar to the other two ranges (II and III) but would cost less. Based on similar spectral range (380–1100 nm), Wu et al. [68] employed hyperspectral imaging to predict moisture content of prawn during dehydration. In their study [68], with the target of extracting the spectra of the whole prawn, both "Manual Prawn Mask" and "Automatic Prawn Mask" were employed to segregate prawns out of homogenous background, as the shape of prawn is irregular. Different from the study of He et al. [45], both linear methods (PLSR and MLR)

and nonlinear method (LS-SVM) were employed to establish the prediction model in the study of Wu et al. [68], coupled with twelve optimal wavelengths selected by successive projections algorithm (SPA). The result showed that SPA-MLR model had similar performance comparing to SPA-PLSR model, but worse than SPA-LS-SVM. However, in the consideration of further industrial applications, SPA-MLR model was selected as the best prediction model with the R_P^2 of 0.962 and ratio of prediction of deviation (RPD) of 4.997.

Table 2 Applications of hyperspectral imaging for detection of chemical attributes of seafood products

Species	Chemical attributes	Spectral range (nm)	Method	R_P^2/R^2	Reference
Prawn	Moisture content	380–1100	PLSR	0.955	Wu et al. [68]
			MLR	0.965	
			LS-SVM	0.984	
Salmon	pH	400–1700	PLSR	0.877	He et al. [10]
	Moisture content	400–1700	PLSR	0.893	He et al. [45]
	Moisture content	900–1700	PLSR	0.887	Fengle et al. [69]
	Fat content			0.865	
	Astaxanthin concentration	385–970	PLSR	0.86	Dissing et al. [51]
	Salt content	760–1040	PLSR	0.74	Segtnan et al. [70]
Grass carp	TVB-N value	400–1000	PLSR	0.891	Cheng et al. [36]
			LS-SVM	0.902	
	TBA value	400–1000	PLSR	0.832	Cheng et al. [43]
			MLR	0.840	
	K value	400–1000	PLSR	0.935	Cheng et al. [44]
			LS-SVM	0.915	

TVB-N total volatile basic nitrogen, *TBA* thiobarbituric acid, *FNN* feed-forward neural network, *PLSR* partial least squares regression, *MLR* multiple linear regression, *LS-SVM* least square support vector machine

Fat and Fatty Acid Content

Fat and fatty acid content are another two important chemical components in meat, having an impact on cooked properties, such as flavor and tenderness. During the past few years, the potential of hyperspectral imaging to predict fat and fatty acids content in muscle foods has been demonstrated. For instance, Kobayashi et al. [61] investigated the relationship between NIR hyperspectral images and fat and fatty acid content of beef by using a methodology that combined NIR hyperspectral imaging (1000–2300 nm) with PLSR. Their study proved that hyperspectral imaging was an effective and advanced method for predicting fat and fatty acid content of beef, with R^2, SEP and RPD of 0.90, 0.87 and 0.89; 4.81, 1.69 and 3.41 %; and 2.84, 2.43 and 2.84 for total fat, saturated fatty acid (SFA) and unsaturated fatty acid (UFA), respectively. All the above results are encouraging, however, for the individual fatty acids, including myristic (C14:0), palmitic (C16:0), stearic (C18:0), myristoleic (C14:1), palmitoleic (C16:1), oleic (C18:1) and linoleic (C18:2) [where C_{xy} indicates the number of carbon atoms (x) and the number of double bonds (y)], and the R^2 and RPD ranged from 0.68 to 0.89 and 1.69 to 2.85, respectively, which was considered not good enough for predicting some individual fatty acids. This is possibly due to the fact that the same regression method is not being able to predict various properties of individual fatty acids. Furthermore, another study [47] also demonstrated the feasibility of hyperspectral imaging for predicting fat content in beef, in which the same method (PLSR) was

applied to establish the model, and satisfactory and comparable results were obtained.

Specifically, intramuscular fat (the amount of fat found between fiber bundles, denoted as IMF), is usually subjectively assessed based on marbling [72]. IMF is significantly related to sensory quality, tenderness and palatability and can play an important role in genetic selection in the meat industry as well. In an early study, Qiao et al. [73] first investigated the relationship between marbling scores of pork and hyperspectral images, using angular second moment (ASM) that defined as a texture index and calculated by gray-level co-occurrence matrix (GLCM) to assess the marbling scores. In their study [73], feed-forward neural network (FNN) models were established for classifying the quality groups of pork samples, with 5 PCs, 10 PCs and 20 PCs, selected from entire spectral wavelengths (430–1000 nm) by PCA, and referenced marbling scores estimated by ASM (ranged from 1.0 to 10.0). The FNN models showed a satisfactory results, yielding correct classification rate (CCR) of 69 % by 5 PCs and 85 % by 10 PCs. For pork, not only quality classification has been made by the marbling scores, but also prediction for the IMF content (assessed by marbling scores) has been carried out. Liu and Ngadi [11] developed hyperspectral imaging to assess IMF content in pork using the wide line detector (WLD), and the WLD-based models have been proved more robust than GLCM-based models [74]. In their study [11], correlation analysis was applied to select the key wavelengths by comparing the Pearson's correlation coefficients, which showed the correlation values between IMF content and spectral feature (MS), 1st

derivative (MS^1) and 2nd derivative (MS^2). Based on the five selected wavelengths, both stepwise regression and PLSR were employed to establish prediction models for analyzing the feasibility of obtaining the proportion of IMF fleck areas (PFA) for predicting IMF content of pork, and MLR models with different entry variables were selected for stepwise procedure. The results showed that PLSR prediction model outperformed the three MLR models, with adjusted R^2 of 0.92 and 0.93 for calibration set and validation set, respectively, which indicated the potential of hyperspectral imaging to predict IMF content in pork with PFA. In addition to pork, hyperspectral imaging was also conducted to determine the marbling content in beef [62].

In addition to beef and pork, fat prediction associating with hyperspectral imaging was carried out in the field of seafood products and showed satisfactory performance. ElMasry and Wold [71] developed hyperspectral imaging in the region of 760–1040 nm to evaluate the fat distribution in six species of fish fillets. In their study, PLSR was applied to establish prediction model with the best number of latent variables (LVs) selected by predicted residual error sum of squares (PRESS) and the selected model performed well with correlation value of 0.91 and RMSECV of 2.99 %. Another study [69], using hyperspectral imaging to assess the fat content of Atlantic salmon fillets in NIR region (899–1649 nm), showed similar performance to the study by ElMasry and Wold [71], with R^2 of 0.93 and RMSEP of 1.24.

pH

pH, as a technological attribute [64], can reflect some chemical attributes of target objects in a way by affecting the activity of microorganisms and has a great influence on color, flavor, water-holding capacity, shelf-life of meat and properties of protein.

Traditionally, pH value of meat is measured by a pH meter or a surface electrode [10]. In the past few years, hyperspectral imaging has been investigated for rapid determination of pH values of meat. In an early study, Qiao et al. [54] determined the pH of pork using a hyperspectral imaging in the spectral region of 430–980 nm, and the six selected wavelengths (494, 571, 637, 69, 703 and 978 nm) show the highest correlation coefficient (r) in simple correlation analysis; however, the FNN model built only achieved a correlation coefficient of 0.55, which is considered not adequate for using in reliable prediction of pH. Recently, a better performed pH prediction model of pork was developed by Barbin et al. [46], who pre-treated all spectra (900–1700 nm) and used PLSR as the regression method to establish prediction model with feature-related wavelengths selected by PLSR-weighted regression coefficients, showing that the model was satisfactory, with R_C^2,

R_P^2, RMSEC and RMSEP being 0.88, 0.90, 0.10 and 0.09, respectively. In addition, another spectral range (400–1000 nm) was employed to predict pH of pork by Pu et al. [56], who used wavelet textural analysis to predict the pH of meat coupled with hyperspectral imaging. In their study, a PLSR model was first established with all spectral data with the purpose of selecting optimal wavelengths, LS-SVM was then applied to establish prediction models with the spectra acquired from feature images, and the best result was obtained when LS-SVM model was established with WT1 (wavelet texture at four level denoted by WT1, WT2, WT3 and WT4), achieving R_C, R_P, RMSEC and RMSEP of 0.964, 0.845, 0.054 and 0.138, respectively. The above two studies [46, 56] employing different spectral range and different analysis methods shows different results, among which the study developed by Barbin et al. [46] showed a better prediction performance. However, it is worth mentioning that wavelet analysis used by Pu et al. [56] is a powerful signal analysis tool for presenting the visual texture of digital images at multiple resolutions [75], which is considered as an important advantage over classical methods as wavelet analysis needs less computational demanding. In addition, wavelets play a role of mathematical functions and are applied to analyze hyperspectral data by disintegrating data into various frequency and components that characterize with a resolution suitable for its scale [56]. Wavelets were first introduced into texture analysis over decades ago [76] and were used to disintegrate texture images that are characterized by first derivative gray-level distribution. Gradually, wavelet analysis has been employed to reduce noise, separate overlapping bands, smooth and correct base line and remove redundancy spectra [26, 77, 78]. Recently, wavelet analysis was also applied in the application of hyperspectral imaging [79], for instance, for the prediction of total volatile basic nitrogen (TVB-N) of prawn [80]. In addition, in the study of Pu et al. [56], wavelet texture analysis, which is usually applied in classification, was employed to fuse both spectral and image features in pH prediction of pork in an attempt to examine its feasibility in such an application, and the results obtained were considered acceptable, showing the potential of wavelet texture analysis to predict pH in pork with hyperspectral images.

In addition to pork, pH determination by hyperspectral imaging was also carried out in meat products; however, published papers in this domain are limited. Iqbal et al. [81] determined pH in cooked and pre-sliced turkey hams by NIR hyperspectral imaging (900–1700 nm). In the study, hyperspectral images of samples were obtained by line-by-line scanning, and based on PLSR analysis, eight optimal wavelengths (927, 947, 1004, 1071, 1121, 1255, 1312 and 1641 nm) were selected, determined by beta coefficients. With the identified optimum wavelengths, PLSR model

was then built for pH prediction with R^2 of 0.81, revealing the robustness of the model for quality assessment in turkey hams.

Similarly, in spite of seafood products that are important sources of human daily diets, little effort was made in pH determination of seafood products with hyperspectral imaging technique. Until recently [10], employed hyperspectral imaging for identifying pH distribution in fresh farmed Atlantic salmons (*Salmon salar*) and the spectral data in visible and near-infrared spectral ranges (400–1700 nm) were collected for subsequent analysis. With the help of PLSR analysis, ten feature-related wavelengths were selected by the means of regression coefficients, and based on these wavelengths, simplified PLSR model was established, yielding R_{CV} of 0.877 and RMSECV of 0.046, which strongly showed the ability of hyperspectral imaging also for pH determination in seafood products.

Protein Content

In addition to moisture, fat and fatty acid, protein is an important functional component of meat as well and has a significant effect on nutritional value and quality of food by affecting their color, flavor and texture, especially on the change of physical and chemical properties of food during processing and storage. On the other hand, the properties of protein are prone to change during storage, due to the activities of microorganism and enzyme, which may cause the loss of nutrition and economic benefit [82]. Therefore, protein content of meat needs to be determined accurately.

Like moisture, the protein content of muscle foods was also assessed in the studies mentioned above, including lamb [20], pork [18] and beef [47]. PLSR was employed to predict protein content of muscle foods in the above three studies, all showing similar satisfactory results, with R_P^2 and SEP of 0.82, 0.88 and 0.86 and 0.47, 0.40 and 0.29 % for lamb, pork and beef, respectively. Among these researches, protein prediction model of pork showed the best R_P^2, while that of beef showed the lowest SEP, which might be due to the different properties and composition of samples. Besides, the prediction of protein content was not only implemented in poultry meats, but also in other meat products, such as ham. Talens et al. [83] developed hyperspectral imaging technique to predict protein content of Spanish cooked hams in NIR spectral region of 900–1700 nm, and PLSR was applied to establish statistical model with ten feature-related wavelengths (930, 971, 1051, 1137, 1165, 1212, 1295, 1400, 1645 and 1682 nm) selected by weighted β-coefficients of PLSR models. Most importantly, the results of the optimal model ($R_{CV}^2 = 0.855$ and RMSECV = 1.09) were good enough to demonstrate the reliability, robustness and accuracy of the

selected model. Simultaneously, based on the information of moisture and protein contents, partial least squares-discriminant analysis (PLS-DA) model was established with the reflectance spectral data to perform classification task. Satisfactorily, the PLS-DA model successfully classified the examined samples into various quality categories, which revealed that protein makes a key contribution to hams classification. The above results indicated the ability of hyperspectral imaging technique for the prediction of protein contents in poultry meats and Spanish cooked hams.

As for seafood products, despite being one of the most important quality protein sources, providing 40 % of protein intake approximately in our diet [84], no studies have been conducted to investigate the ability of hyperspectral imaging technique for the identification of protein content of seafood products. Therefore, relevant studies need to be developed, including prediction of some individual protein or amino acids. It is worth mentioning that the potential of hyperspectral imaging for predicting individual amino acids content, hydroxyproline, in chicken meat has been successfully investigated by Xiong et al. [48], with R_P of 0.854 and RMSEP of 0.049.

Pigment

Apparently, satisfactory color meats, reflecting good quality and freshness, are attractive to customers more than pale color meats, and pigments make a significant contribution to the color of meats; for instance, astaxanthin and castaxanthin, two natural carotenoids existing in salmons, oysters, trouts or the shell of prawns [51], work as antioxidant to keep a bright color of seafood products. Therefore, a number of researchers have made effort to measure the pigments of meats with hyperspectral imaging.

With regard to poultry meats, Xiong et al. [63] used hyperspectral imaging technique to determine total pigments in poultry meats, including goose, beef and duck, in the range of 400–1000 nm, and MSC, SPA and PLSR were applied to pre-treat spectral data, select seven optimal wavelengths and establish prediction model, respectively. Fortunately, SPA-PLSR model was reliable, robust and stable, with R_P^2 of 0.953, RMSEP of 9.896 and RPD of 4.628. Apparently, the high R_P^2 and RPD value revealed the excellent performance of the model. However, the RMSEP value, which is expected to be low, was actually high at the same time, which might relate with different levels of pigments in three different types of meats.

At the same time, relevant studies for pigments prediction, especially for astaxanthin, were carried out in aquaculture. The first attempt, integrating hyperspectral imaging technique with astaxanthin concentration prediction in rainbow trout fillets, was made by Dissing et al.

[51]. This study successfully proved the ability of hyperspectral imaging for astaxanthin prediction by using PLSR to calibrate model, with R_P^2 of 0.86 and RMSEP of 0.27 for multispectral imaging and RGB imaging, respectively. However, very few researches about pigments prediction of seafood products by hyperspectral imaging have been reported, and thus, more studies should be conducted in this area in future.

Salt Content

It is known that salt content is of great importance to perceived saltiness, quality and shelf-life of processed meats, for the reason that it works as flavor modifier and microbial inhibitor. However, high level of salt has received negative reports, because of its apparent harm for cardiovascular system of human [50]. Although hyperspectral imaging could be used to detect salt content, very few studies were conducted in the area probably due to that salt content can only be predicted indirectly as absorption bands of NaCl cannot be collected in the region of NIR wavelength [85]. A research developed by Liu et al. [50] proved the feasibility of hyperspectral imaging for predicting salt content in porcine meat, in which three linear algorithms, including PLSR, PCR and MLR, were employed to develop model with six key wavelengths selected by PLSR-weighted regression coefficients, respectively. After comparing the above three models, MLR model was selected as the best calibration model to visualize the salt content of porcine meat, with R_P^2 of 0.930 and RMSEP of 0.682. Another study about prediction of salt content in dry-cured ham slices was developed by Gou et al. [49], in which acceptable results were also obtained.

In the case of seafood products, an analysis about salt distribution in salted and smoked salmon fillets using NIR interactance imaging was done by Segtnan et al. [70]. In this research, PLSR calibration model was established with referenced NaCl values and average NIR spectra pre-treated by SNV, yielding an RMECV of 0.56 and an R of 0.86, which was considered as acceptable.

Freshness Attributes

Freshness attributes, immediately reflecting the change or the reaction of chemical composition of muscle foods, belong to chemical attributes and are significant for both consumers and industrial merchants, as abundant nutritional composition in muscle foods is sensitive to the biochemical activities internally, which affects freshness and quality of meat. In fact, there are various indexes that can reflect freshness of meat, including TBA, K value, trimethylamine (TMA), biogenic amines and TVB-N. However, up to now, only a few studies have been

conducted that using hyperspectral imaging for TVB-N, TBA and K value determination.

TVB-N, defined as a kind of alkali compound containing nitrogen, appearing during the decomposition of protein, is considered as an effective index to assess the freshness of meat. In recent years, some researchers have devoted effort to determine TVB-N. Chen et al. [58] demonstrated that hyperspectral imaging was a promising tool for TVB-N determination with a suitable hypercube processing algorithm in pork in jelly. In their study [58], a back-propagation artificial neural network (BP-ANN) coupled with PCA was used to construct prediction model of TVB-N with fusion data, and the final model achieved a satisfactory result with R_P of 0.8334. However, the algorithm employed in the above study was simple and lacked comparison to show the superiority of BP-ANN. Hence, both Cheng et al. [36] and Dai et al. [86] employed hyperspectral imaging technique (400–1000 nm) with more robust algorithms, including LS-SVM, PLSR, Ada-Boost and BP-ANN in TVB-N prediction of grass craps (Ctenopharyngodon idella) or freshness classification of prawns based on TVB-N value, and both studies showed that LS-SVM model had better performance than other models, with R_P^2 of 0.902 for TVB-N prediction in grass carp and CCR 98.33 and 95 % for frozen and unfrozen groups in classification of prawns, respectively.

TBA can also reflect the freshness of meat by determining the level of lipid oxidation during storage, and higher TBA value indicates lower freshness and worse quality. Recently, investigations about TBA prediction using hyperspectral imaging have been extended to poultry meat and seafood products. For instance, the prediction of thiobarbituric acid reactive substances (TBARS) was developed with hyperspectral imaging by Xiong et al. [67], in which SPA-PLSR was selected as the optimal model to visualize TBARS content in the chicken meat, showing an encouraging result with R_P of 0.801 and RMSEP of 0.157. At the same time, Cheng et al. [43] developed a laboratory push-broom hyperspectral imaging system to determine TBA in grass carp (Ctenopharyngodon idella), constructed PLSR and MLR models with ten optimal wavelengths (444, 475, 553, 577, 590, 623, 710, 795, 847 and 937 nm) selected by weighted regression coefficients and showed that the best result was achieved from the MLR model, with R_P^2 of 0.8395 and RMSEP of 0.1147.

In addition to TVB-N and TBA, K value is another attribute widely used to determine the freshness of seafood products by indicating nucleotide degradation, which has a great impact on the flavor of seafood products. K value can reflect the quantitative relation of adenosine 50-triphosphate (ATP) and its corresponding series of breakdown products, including adenosine 50-diphosphate (ADP), adenosine 50-monophosphate (AMP), inosine 50-

monophosphate (IMP), inosine (HxR) and hypoxhantine (Hx) [87], and is usually calculated as the ratio of HxR and Hx to the sum of ATP and all the degradation products and expressed as follows:

$$K = \frac{HxR + Hx}{ATP + ADP + AMP + IMP + HxR + Hx} \times 100 \%$$

(3)

Up to now, only one study [44] was available, in which the feasibility of hyperspectral imaging for identification of K value of fish fillets was investigated, and both linear (PLSR) and nonlinear algorithms (LS-SVM) were applied to establish models with both full wavelengths and seven optimal wavelengths (432, 455, 588, 635, 750, 840 and 970 nm) in the region of 400–1000 nm. After comparison, the PLSR model established with the seven optimal wavelengths was selected as the best model and was used to generate chemical map, with R_P^2 of 0.935 and RMSEP of 0.0517. For the first time, this study indicated the possibility of hyperspectral imaging for prediction of K value in muscle foods.

Advantages and Future Trends

Based upon the above studies, it has been confirmed that hyperspectral imaging is an available and alternative technique for rapidly and nondestructively identifying chemical composition of muscle foods. Different from traditional methods, the measurements using hyperspectral imaging technique is chemical-free, nondestructive, time-saving and environmentally friendly. In addition, hyperspectral imaging technique overcomes the limitation of individual technique of spectroscopy and computer vision, which means that it can simultaneously obtain both spectral and spatial information of the samples. Most importantly, it provides means to visualize the concentration of chemical composition through chemical mapping, using color scale to indicate concentration gradient in the chemical map. For practical application, hyperspectral imaging technique can be implemented as an innovative technological tool to accomplish quantitative identification and qualitative analysis; for industrial application, it can realize rapid detection and real-time information collection.

On the other hand, like other novel technologies, hyperspectral imaging technique is no doubt possessing some disadvantages that need to be overcome in further studies as discussed below.

- At present, optimal wavelengths containing most valuable information of the quality attributes need to be selected manually, which takes time and reduces processing efficiency. Therefore, future studies can develop algorithms for automatic selection of optimal wavelengths for use in establishing model directly.

- Most studies employ regular linear regression algorithms, including PLSR, MLR, and PCA, and more nonlinear algorithms and new regression algorithms need to be developed for enhancing model performance and robustness.

- Current configurations of hyperspectral imaging cannot be employed directly in the industry as it cannot meet the current requirements in on-line industrial settings due to the following reasons. Firstly, hyperspectral images contain a significant number of redundant data, which can slow down the image processing rate; secondly, although there are a number of models available for quality attribute prediction, these models are normally established based on single quality attribute and thus cannot be used for the prediction of multiple quality attributes, therefore a number of models will be needed, and alternatively efforts should be made to develop models that can predict multiple quality attributes; and finally, the cost for hyperspectral imaging instruments are still high, and low cost instruments should be developed.

- For industrial applications, efforts should be made to make multispectral imaging technology widely available for the food industry.

Conclusions

This review first introduced the principles of hyperspectral imaging, and its hardware, software requirements and relevant chemometrics. The applications of hyperspectral imaging in identifying chemical composition of meat are then thoroughly discussed, including moisture content, fat and fatty acid contents, pH, protein content, pigments, salt content and some freshness attributes. It is shown that hyperspectral imaging, as a rapid and noninvasive technique, is able to obtain both spectral information and images simultaneously. However, some obstacles still need to be overcome, such as the redundant information from full wavelengths, and the limited number of regression algorithms available. With the development of computing and chemometric techniques, it is expected that hyperspectral or multispectral imaging technique should find wider applications in the food industry in future.

References

1. Zheng LY, Sun D-W (2004) Vacuum cooling for the food industry: a review of recent research advances. Trends Food Sci Technol 15(12):555–568
2. Wang LJ, Sun D-W (2004) Effect of operating conditions of a vacuum cooler on cooling performance for large cooked meat joints. J Food Eng 61(2):231–240
3. Sun D-W, Wang LJ (2000) Heat transfer characteristics of cooked meats using different cooling methods. Int J Refrig 23(7):508–516
4. Desmond EM, Kenny TA, Ward P, Sun D-W (2000) Effect of rapid and conventional cooling methods on the quality of cooked ham joints. Meat Sci 56(3):271–277
5. Kiani H, Zhang Z, Delgado A, Sun D-W (2011) Ultrasound assisted nucleation of some liquid and solid model foods during freezing. Food Res Int 44(9):2915–2921
6. Cui Z-W, Sun L-J, Chen W, Sun D-W (2008) Preparation of dry honey by microwave-vacuum drying. J Food Eng 84(4):582–590
7. Delgado AE, Sun D-W (2002) Desorption isotherms and glass transition temperature for chicken meat. J Food Eng 55(1):1–8
8. Huang H, Liu L, Ngadi MO (2014) Recent developments in hyperspectral imaging for assessment of food quality and safety. Sensors 14(4):7248–7276
9. Petracci M, Baeza E (2011) Harmonization of methodologies for the assessment of poultry meat quality features. Worlds Poult Sci J 67(1):137–151
10. He H-J, Wu D, Sun D-W (2014) Rapid and non-destructive determination of drip loss and pH distribution in farmed Atlantic salmon (Salmo salar) fillets using visible and near-infrared (Vis–NIR) hyperspectral imaging. Food Chem 156:394–401
11. Liu L, Ngadi MO (2014) Predicting intramuscular fat content of pork using hyperspectral imaging. J Food Eng 134:16–23
12. Wu D, Sun D-W (2013) Colour measurements by computer vision for food quality control: a review. Trends Food Sci Technol 29(1):5–20
13. Jackman P, Sun D-W, Du C-J, Allen P (2009) Prediction of beef eating qualities from colour, marbling and wavelet surface texture features using homogenous carcass treatment. Pattern Recognit 42(5):751–763
14. Wang HH, Sun D-W (2002) Melting characteristics of cheese: analysis of effect of cheese dimensions using computer vision techniques. J Food Eng 52(3):279–284
15. Jackman P, Sun D-W, Allen P (2009) Automatic segmentation of beef longissimus dorsi muscle and marbling by an adaptable algorithm. Meat Sci 83(2):187–194
16. Xiong Z, Sun D-W, Zeng X-A, Xie A (2014) Recent developments of hyperspectral imaging systems and their applications in detecting quality attributes of red meats: a review. J Food Eng 132:1–13
17. Chen Q, Zhang C, Zhao J, Ouyang Q (2013) Recent advances in emerging imaging techniques for non-destructive detection of food quality and safety. Trac Trends Anal Chem 52:261–274
18. Barbin DF, ElMasry G, Sun D-W, Allen P (2013) Non-destructive determination of chemical composition in intact and minced pork using near-infrared hyperspectral imaging. Food Chem 138(2–3):1162–1171
19. Elmasry G, Barbin DF, Sun D-W, Allen P (2012) Meat quality evaluation by hyperspectral imaging technique: an overview. Crit Rev Food Sci Nutr 52(8):689–711
20. Kamruzzaman M, ElMasry G, Sun D-W, Allen P (2012) Non-destructive prediction and visualization of chemical composition in lamb meat using NIR hyperspectral imaging and multivariate regression. Innov Food Sci Emerg Technol 16:218–226
21. Barbin D, ElMasry G, Sun D-W, Allen P (2012) Near-infrared hyperspectral imaging for grading and classification of pork. Meat Sci 90(1):259–268
22. ElMasry G, Kamruzzaman M, Sun D-W, Allen P (2012) Principles and applications of hyperspectral imaging in quality evaluation of agro-food products: a review. Crit Rev Food Sci Nutr 52(11):999–1023
23. Wu D, Sun D-W, He Y (2012) Application of long-wave near infrared hyperspectral imaging for measurement of color distribution in salmon fillet. Innov Food Sci Emerg Technol 16:361–372
24. Wu D, Sun D-W (2013) Potential of time series-hyperspectral imaging (TS-HSI) for non-invasive determination of microbial spoilage of salmon flesh. Talanta 111:39–46
25. Feng Y-Z, Sun D-W (2012) Application of hyperspectral imaging in food safety inspection and control: a review. Crit Rev Food Sci Nutr 52(11):1039–1058
26. Liu D, Sun D-W, Zeng X-A (2014) Recent advances in wavelength selection techniques for hyperspectral image processing in the food industry. Food Bioprocess Technol 7(2): 307–323
27. Feng Y-Z, Sun D-W (2013) Near-infrared hyperspectral imaging in tandem with partial least squares regression and genetic algorithm for non-destructive determination and visualization of Pseudomonas loads in chicken fillets. Talanta 109:74–83
28. Feng Y-Z, ElMasry G, Sun D-W, Scannell AGM, Walsh D, Morcy N (2013) Near-infrared hyperspectral imaging and partial least squares regression for rapid and reagentless determination of Enterobacteriaceae on chicken fillets. Food Chem 138(2–3): 1829–1836
29. Goetz AF, Vane G, Solomon JE, Rock BN (1985) Imaging spectrometry for Earth remote sensing. Science 228(4704):1147–1153
30. Wu D, Sun D-W (2013) Advanced applications of hyperspectral imaging technology for food quality and safety analysis and assessment: a review-part II—applications. Innov Food Sci Emerg Technol 19:15–28
31. Lorente D, Aleixos N, Gómez-Sanchis J, Cubero S, García-Navarrete O-L, Blasco J (2012) Recent advances and applications of hyperspectral imaging for fruit and vegetable quality assessment. Food Bioprocess Technol 5(4):1121–1142
32. Cheng J-H, Sun D-W (2015) Rapid quantification analysis and visualization of Escherichia coli loads in grass carp fish flesh by hyperspectral imaging method. Food Bioprocess Technol 8(5): 951–959
33. Zhu F, Zhang D, He Y, Liu F, Sun D-W (2013) Application of visible and near infrared hyperspectral imaging to differentiate between fresh and frozen–thawed fish fillets. Food Bioprocess Technol 6(10):2931–2937
34. Gowen AA, O'Donnell CP, Cullen PJ, Downey G, Frias JM (2007) Hyperspectral imaging—an emerging process analytical tool for food quality and safety control. Trends Food Sci Technol 18(12):590–598
35. Qin JW, Chao KL, Kim MS, Lu RF, Burks TF (2013) Hyperspectral and multispectral imaging for evaluating food safety and quality. J Food Eng 118(2):157–171
36. Cheng J-H, Sun D-W, Zeng X-A, Pu H-B (2014) Non-destructive and rapid determination of TVB-N content for freshness evaluation of grass carp (Ctenopharyngodon idella) by hyperspectral imaging. Innov Food Sci Emerg Technol 21:179–187
37. Wu D, Sun D-W (2013) Advanced applications of hyperspectral imaging technology for food quality and safety analysis and assessment: a review-part I—fundamentals. Innov Food Sci Emerg Technol 19:1–14

38. Zeaiter M, Roger JM, Bellon-Maurel V, Rutledge DN (2004) Robustness of models developed by multivariate calibration. Part I: the assessment of robustness. TrAC Trends Anal Chem 23(2):157–170

39. Prats-Montalbán JM, de Juan A, Ferrer A (2011) Multivariate image analysis: a review with applications. Chemometr Intell Lab Syst 107(1):1–23

40. Wold S, Sjöström M, Eriksson L (2001) PLS-regression: a basic tool of chemometrics. Chemometr Intell Lab Syst 58(2):109–130

41. Agatonovic-Kustrin S, Beresford R (2000) Basic concepts of artificial neural network (ANN) modeling and its application in pharmaceutical research. J Pharm Biomed Anal 22(5):717–727

42. Zhang L, Zhou W, Jiao L (2004) Wavelet support vector machine. IEEE Trans Syst Man Cybernet B (Cybernetics) 34(1):34–39

43. Cheng J-H, Sun D-W, Pu H-B, Wang Q-J, Chen Y-N (2015) Suitability of hyperspectral imaging for rapid evaluation of thiobarbituric acid (TBA) value in grass carp (Ctenopharyngodon idella) fillet. Food Chem 171:258–265

44. Cheng J-H, Sun D-W, Pu H, Zhu Z (2015) Development of hyperspectral imaging coupled with chemometric analysis to monitor K value for evaluation of chemical spoilage in fish fillets. Food Chem 185:245–253

45. He H-J, Wu D, Sun D-W (2013) Non-destructive and rapid analysis of moisture distribution in farmed Atlantic salmon (Salmo salar) fillets using visible and near-infrared hyperspectral imaging. Innova Food Sci Emerg Technol 18:237–245

46. Barbin DF, ElMasry G, Sun D-W, Allen P (2012) Predicting quality and sensory attributes of pork using near-infrared hyperspectral imaging. Anal Chim Acta 719:30–42

47. ElMasry G, Sun D-W, Allen P (2013) Chemical-free assessment and mapping of major constituents in beef using hyperspectral imaging. J Food Eng 117(2):235–246

48. Xiong ZJ, Sun D-W, Xie AG, Han Z, Wang L (2015) Potential of hyperspectral imaging for rapid prediction of hydroxyproline content in chicken meat. Food Chem 175:417–422

49. Gou P, Santos-Garcés E, Høy M, Wold JP, Liland KH, Fulladosa E (2013) Feasibility of NIR interactance hyperspectral imaging for on-line measurement of crude composition in vacuum packed dry-cured ham slices. Meat Sci 95(2):250–255

50. Liu D, Qu J, Sun D-W, Pu H, Zeng X-A (2013) Non-destructive prediction of salt contents and water activity of porcine meat slices by hyperspectral imaging in a salting process. Innov Food Sci Emerg Technol 20:316–323

51. Dissing BS, Nielsen ME, Ersboll BK, Frosch S (2011) Multispectral imaging for determination of Astaxanthin concentration in salmonids. PLoS One 6(5):e19032

52. Cheng J-H, Sun D-W (2014) Hyperspectral imaging as an effective tool for quality analysis and control of fish and other seafoods: current research and potential applications. Trends Food Sci Technol 37(2):78–91

53. Karoui R, Mouazen AM, Dufour E, Pillonel L, Picque D, Bosset JO et al (2006) Mid-infrared spectrometry: a tool for the determination of chemical parameters in Emmental cheeses produced during winter. Lait 86:83–97

54. Qiao J, Wang N, Ngadi MO, Gunenc A, Monroy M, Gariépy C, Prasher SO (2007) Prediction of drip-loss, pH, and color for pork using a hyperspectral imaging technique. Meat Sci 76(1):1–8

55. Liu D, Pu H, Sun D-W, Wang L, Zeng X-A (2014) Combination of spectra and texture data of hyperspectral imaging for prediction of pH in salted meat. Food Chem 160:330–337

56. Pu H, Sun D-W, Ma J, Liu D, Cheng J-H (2014) Using wavelet textural features of visible and near infrared hyperspectral image to differentiate between fresh and Frozen-Thawed Pork. Food Bioprocess Technol 7(11):3088–3099

57. Xie A, Sun D-W, Xu Z, Zhu Z (2015) Rapid detection of frozen pork quality without thawing by Vis–NIR hyperspectral imaging technique. Talanta 139:208–215

58. Chen QS, Zhang YH, Zhao JW, Hui Z (2013) Nondestructive measurement of total volatile basic nitrogen (TVB-N) content in salted pork in jelly using a hyperspectral imaging technique combined with efficient hypercube processing algorithms. Anal Methods 5(22):6382–6388

59. Kim MS, Li Y, Zhang L, Peng Y, Tang X, Chao K, Dhakal S, Tu SI, Chao K (2011) Hyperspectral imaging technique for determination of pork freshness attributes 8027, 80270H-80270H-80279

60. ElMasry G, Sun D-W, Allen P (2012) Near-infrared hyperspectral imaging for predicting colour, pH and tenderness of fresh beef. J Food Eng 110(1):127–140

61. Kobayashi K-I, Matsui Y, Maebuchi Y, Toyota T, Nakauchi S (2010) Near infrared spectroscopy and hyperspectral imaging for prediction and visualisation of fat and fatty acid content in intact raw beef cuts. J Near Infrared Spectrosc 18(5):301–315

62. Li Y, Shan J, Peng Y, Gao X (2011) Nondestructive assessment of beef-marbling grade using hyperspectral imaging technology. In: IEEE 2011 international conference on new technology of agricultural engineering (ICAE), pp 779–783

63. Xiong Z, Sun D-W, Xie A, Pu H, Han Z, Luo M (2015) Quantitative determination of total pigments in red meats using hyperspectral imaging and multivariate analysis. Food Chem 178:339–345

64. Kamruzzaman M, ElMasry G, Sun D-W, Allen P (2012) Prediction of some quality attributes of lamb meat using near-infrared hyperspectral imaging and multivariate analysis. Anal Chim Acta 714:57–67

65. Pu H, Sun D-W, Ma J, Liu D, Kamruzzaman M (2014) Hierarchical variable selection for predicting chemical constituents in lamb meats using hyperspectral imaging. J Food Eng 143:44–52

66. Kandpal LM, Lee H, Kim MS, Mo C, Cho B-K (2013) Hyperspectral reflectance imaging technique for visualization of moisture distribution in cooked chicken breast. Sensors 13(10):13289–13300

67. Xiong Z, Sun D-W, Pu H, Xie A, Han Z, Luo M (2015) Nondestructive prediction of thiobarbituric acid reactive substances (TBARS) value for freshness evaluation of chicken meat using hyperspectral imaging. Food Chem 179:175–181

68. Wu D, Shi H, Wang SJ, He Y, Bao YD, Liu KS (2012) Rapid prediction of moisture content of dehydrated prawns using online hyperspectral imaging system. Anal Chim Acta 726:57–66

69. Fengle Z, Hailiang Z, Yongni S, Yong H, Ngadi M (2014) Mapping of fat and moisture distribution in atlantic salmon using near-infrared hyperspectral imaging. Food Bioprocess Technol 7(4):1208–1214

70. Segtnan VH, Hoy M, Sorheim O, Kohler A, Lundby F, Wold JP, Ofstad R (2009) Noncontact salt and fat distributional analysis in salted and smoked salmon fillets using X-ray computed tomography and NIR interactance imaging. J Agric Food Chem 57(5):1705–1710

71. ElMasry G, Wold JP (2008) High-speed assessment of fat and water content distribution in fish fillets using online imaging spectroscopy. J Agric Food Chem 56(17):7672–7677

72. Thaller G, Kühn C, Winter A, Ewald G, Bellmann O, Wegner J, Zühlke H, Fries R (2003) DGAT1, a new positional and functional candidate gene for intramuscular fat deposition in cattle. Anim Genet 34(5):354–357

73. Qiao J, Ngadi MO, Wang N, Gariépy C, Prasher SO (2007) Pork quality and marbling level assessment using a hyperspectral imaging system. J Food Eng 83(1):10–16

74. Huang H, Liu L, Ngadi M, Gariepy C (2013) Prediction of pork marbling scores using pattern analysis techniques. Food Control 31(1):224–229

75. Dai Q, Cheng JH, Sun DW, Zeng XA (2015) Advances in feature selection methods for hyperspectral image processing in food

industry applications: a review. Crit Rev Food Sci Nutr 55(10): 1368–1382

76. Mallat Stephane G (1989) A theory for multiresolution signal decomposing: the wavelet representation. IEEE Trans PAMI 11(7):674–693

77. Barclay VJ, Bonner RF, Hamilton IP (1997) Application of wavelet transforms to experimental spectra: smoothing, de-noising, and data set compression. Anal Chem 69:78–90

78. Gributs CEW, Burns DH (2006) Parsimonious calibration models for nearinfrared spectroscopy using wavelets and scaling functions. Chemometr Intell Lab Syst 83:44–53

79. Singh C-B, Choudhary R, Jayas D-S, Paliwal J (2010) Wavelet analysis of signals in agriculture and food quality inspection. Food Bioprocess Technol 3(1):2–12

80. Dai Q, Cheng JH, Sun DW, Zhu Z, Pu H (2016) Prediction of total volatile basic nitrogen contents using wavelet features from visible/near-infrared hyperspectral images of prawn (Metapenaeus ensis). Food Chem 197:257–265

81. Iqbal A, Sun D-W, Allen P (2013) Prediction of moisture, color and pH in cooked, pre-sliced turkey hams by NIR hyperspectral imaging system. J Food Eng 117(1):42–51

82. Badii F, Howell NK (2002) Effect of antioxidants, citrate, and cryoprotectants on protein denaturation and texture of frozen cod (Gadus morhua). J Agric Food Chem 50(7):2053–2061

83. Talens P, Mora L, Morsy N, Barbin DF, ElMasry G, Sun D-W (2013) Prediction of water and protein contents and quality classification of Spanish cooked ham using NIR hyperspectral imaging. J Food Eng 117(3):272–280

84. Cheng J-H, Dai Q, Sun D-W, Zeng X-A, Liu D, Pu H-B (2013) Applications of non-destructive spectroscopic techniques for fish quality and safety evaluation and inspection. Trends Food Sci Technol 34(1):18–31

85. Begley TH, Lanza E, Norris KH, Hruschka WR (1984) Determination of sodium chloride in meat by near-infrared diffuse reflectance spectroscopy. J Agric Food Chem 32(5):984–987

86. Dai Q, Cheng J-H, Sun D-W, Pu H, Zeng X-A, Xiong Z (2015) Potential of visible/near-infrared hyperspectral imaging for rapid detection of freshness in unfrozen and frozen prawns. J Food Eng 149:97–104

87. Lowe T, Ryder J, Carragher J, Wells R (1993) Flesh quality in snapper, Pagrcrs auratus, affected by capture stress. J Food Sci 58(4):770–773